Optical studies of lithium vapour zones produced by thermal evaporation in noble gas

1997 J. Phys.: Condens. Matter 9 5801

(http://iopscience.iop.org/0953-8984/9/27/011)

J. Phys.: Condens. Matter **9** (1997) 5801–5814. Printed in the UK PII: S0953-8984(97)80325-6

Optical studies of lithium vapour zones produced by thermal evaporation in noble gas

Shosuke Mochizuki†§, Mie Sasaki† and Raphael Ruppin‡

† Department of Physics, College of Humanities and Sciences, Nihon University, 3-25-40 Sakurajosui, Setagaya-ku, Tokyo 156, Japan

‡ Department of Physics and Applied Mathematics, SOREQ NRC, Yavne 81800, Israel

Received 17 December 1996, in final form 15 April 1997

Abstract. We have produced two vertically well separated zones of lithium vapour above the evaporation source in a confined noble gas atmosphere by setting an appropriate condition for the gas evaporation. Optical extinction spectra of lithium atoms, dimers and clusters were obtained by time-resolved and space-resolved measurements after the beginning of the evaporation. Also, vapour species in each zone were selectively excited using laser light and the emission spectra were measured. Some of the observed spectra were compared with theoretical ones, and information on the following points was derived: (i) the mechanism of lithium cluster and microcrystal growth in the gas evaporation method, (ii) the size trend of the collective mode resonance of the valence electrons, (iii) the excitation energy transfer between lithium vapour species, (iv) the structure of the vapour zone and (v) the mechanism of laser photofragmentation of clusters.

1. Introduction

It is well known that clusters and microcrystals can be produced easily by thermal evaporation under a low-pressure noble gas (Ueda 1974). This method is called the 'gas evaporation method'. On the growth mechanism of clusters and microcrystals, several models have been reported, but the following basic problems still remain to be confirmed experimentally. (i) What species (atoms, dimers or clusters) evaporate from the melted surface? (ii) How do the evaporated species aggregate and how do they cool down and stabilize?

In order to elucidate the problems of gas evaporation by optical methods, a simple vapour zone should be established. Recently, we have produced two vertically well separated zones of various metals (Na, K, Rb, Cu, Ag and Au) above the evaporation source in a confined He gas atmosphere by setting an appropriate condition for the gas evaporation and obtained the optical extinction spectra as a function of the time elapsed after the beginning of evaporation and of the height from the upper edge of the evaporation source (Mochizuki 1993, Mochizuki and Ruppin 1993, 1994). The structure of the spectra and their dependence on time on the one hand, and on the distance from the evaporation source on the other hand, indicate that the species evaporated from the melted surface are atoms, which then dimerize and grow into clusters by coalescence with other atoms. Here we apply this technique to lithium, which is of special interest, because the deviation of its properties from those predicted by the nealy-free-electron model are much larger than for the other alkali metals.

§ E-mail address: motizuki@physics.chs.nihon-u.ac.jp

0953-8984/97/275801+14$19.50

Also, we excited selectively dimers and clusters in lithium vapour zones by laser light and measured their emissions (Mochizuki and Sasaki 1995). The results gave information on the interaction between vapour species. With increasing laser fluence, the photofragmentation phenomenon becomes prominent. In the laser photofragmentation of the vapour zones of sodium, potassium and rubidium, we frequently observed diffuse bands, which may arise from dissociation of trimers to produce excimer-like dimers (Mochizuki and Sasaki 1996). Therefore, such laser-photofragmentation spectroscopy may give more detailed information on the vapour zones, which complements what the extinction measurements give. However, the following basic problems of the laser photofragmentation still remain to be explored experimentally. (i) How does the target absorb the incident photon energy? (ii) How does the energy absorbed redistribute into other degrees of freedom within the target system, and how does the energy concentrate on a special mode to emit particles? (iii) What particles are emitted directly from target surface? (iv) How do the emitted particles aggregate or fragment, and how do they cool down to become stable? In order to establish the measurement method of the vapour zones using the laser photofragmentation spectroscopy, these problems should be clarified.

In the present paper, we report the details of our experiments on lithium and identify the various features appearing in the optical spectra. The experiments on the laser photofragmentation of lithium vapour are also reported.

2. Experimental details

2.1. Gas evaporation experiments

Gas evaporation experiments were carried out using the apparatus described earlier (Mochizuki and Ruppin 1993). A stainless steel crucible containing nominally pure lithium metal was gradually heated indirectly in an alumina crucible on which a tungsten-wire heater was wound. Figure 1 shows a typical view of the gas evaporation of lithium in helium gas confined at 150 Torr. This photograph was taken at the middle stage of gas evaporation with illumination of a xenon lamp. A dark faint red zone (DZ) ranging from the upper edge of the crucible (C) to a height of about 5 mm, and a long conical blue zone (BZ) can be clearly distinguished. As shown at a later section, the dark faint red and blue colours correspond to the fluorescence of lithium atoms and the collective mode resonance scattering of lithium clusters, respectively. As the gas evaporation proceeds, the blue zone grows to produce a multilayer cone structure. Optical extinction spectra of selected positions in the vapour zones were recorded in the transmission configuration as a function of the time elapsed from the beginning of the evaporation. All the extinction spectra presented here display the quantity $-\log T_r$, where T_r is the intensity ratio of the transmitted radiation during the evaporation process to that of the transmitted radiation through the same position before the beginning of the gas evaporation. In addition, the emission spectra of selected positions were recorded in the right-angle scattering configuration. The emitted light was dispersed using a grating spectrograph (Jobin–Yvon HR-320), and a multichannel-photodetection system was employed. The excitations were carried out using several argon ion laser lines and a nitrogen molecular laser line. Optical spectra were measured with an optical multichannel analyser.

Apart from the evaporation in confined atmospheric gas, and in order to measure the optical extinction spectra of microcrystals up to the large-size region, evaporation was also carried out in a low-pressure gas stream which was produced by supplying helium gas to the bottom of the evaporation chamber and pumping it with a mechanical booster pump

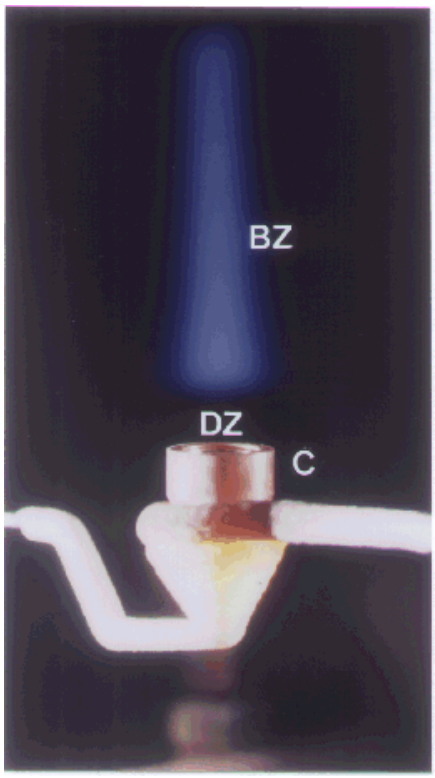

Figure 1. A typical view of gas evaporation of lithium. Gas evaporation was carried out in helium gas confined at 150 Torr.

(exhaust speed of 800 l min^{-1}). The chamber, evaporation source and optical system were the same as those used for the confined atmosphere experiments.

In the experiments under both the confined and flowing gas conditions, we determined the temperatures of vapour zones with a thermocouple as functions of height and time elapsed after starting of heating.

2.2. Laser photofragmentation experiments

The experiments were carried out by using a Nd^{3+}–YAG laser line ($\lambda = 1.06$ μm; fluence, 200 mJ cm^{-2}; pulse width, 10 ns or 5 μs) on lithium vapour produced by gas evaporation. The diameter of the laser spot was 0.6 mm. The emitted light was dispersed using a grating spectrograph (Jobin–Yvon HR-320) and a multichannel-photodetection system was employed. After an intense laser light pulse, the emissions from the target vapour were recorded in the right-angle scattering configuration. Unfortunately, our measurement system has a large fluctuation (several hundred nanoseconds) in the repetition time of the laser oscillation, and an inherent time delay (85 ns) of the delay pulse generator which is used to activate the detection system in the time-resolved measurement mode. Thus, the emission with short delay time ($\ll 85$ ns) and the time evolution of photofragmentation could not be observed. Therefore, in order to observe reliable photofragmentaion emission from vapour species, we excited the laser light with a pulse of 5 μs and measured emission with an integration time of 1 s. The integration was started just before the laser irradiation.

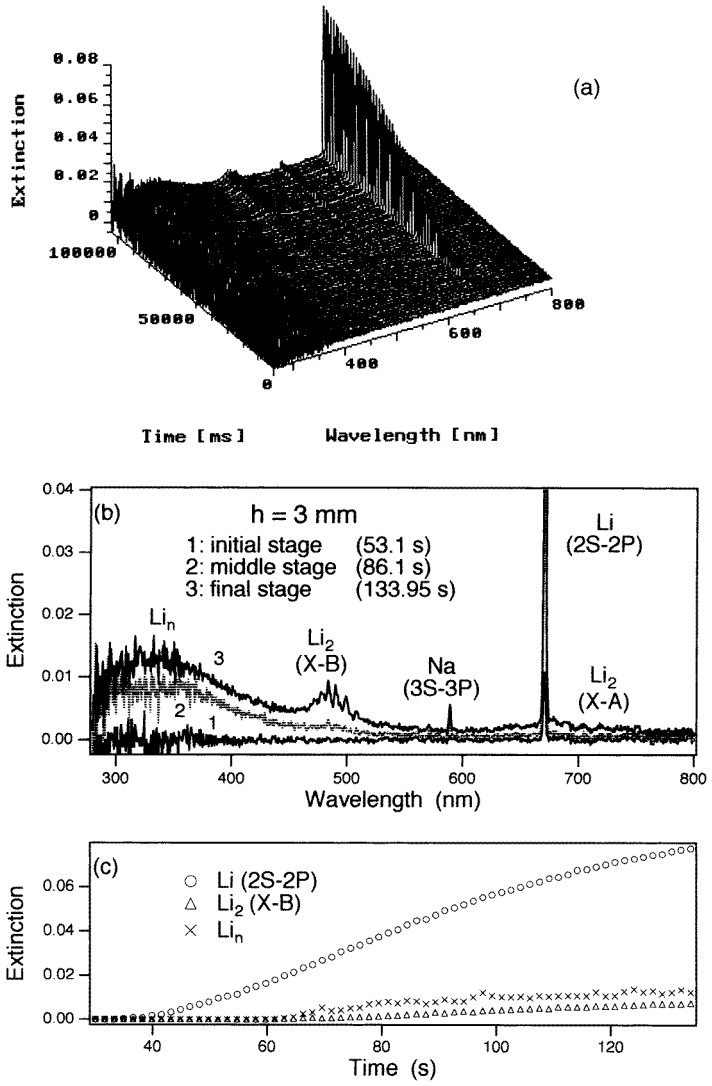

Figure 2. Extinction spectra of the lithium vapour zone at a height of 3 mm from the crucible: (a) time evolution of the extinction spectrum; (b) extinction spectra at the initial, middle and final stages of evaporation; (c) the time dependences of the extinctions due to lithium atoms, dimers and clusters.

3. Results and discussion

3.1. Optical extinction spectra of the lithium vapour zone

Figure 2(a) shows the time evolution of the extinction spectrum of the dark faint red zone at a height of 3 mm from the crucible edge at 150 Torr. The optical measurements began 30 s after the beginning of the heating. In figure 2(b), the spectra at the initial, middle and final stages of gas evaporation are shown. The times indicated are the times elapsed after the beginning of the heating. During the gas evaporation, the temperatures of the measured zone

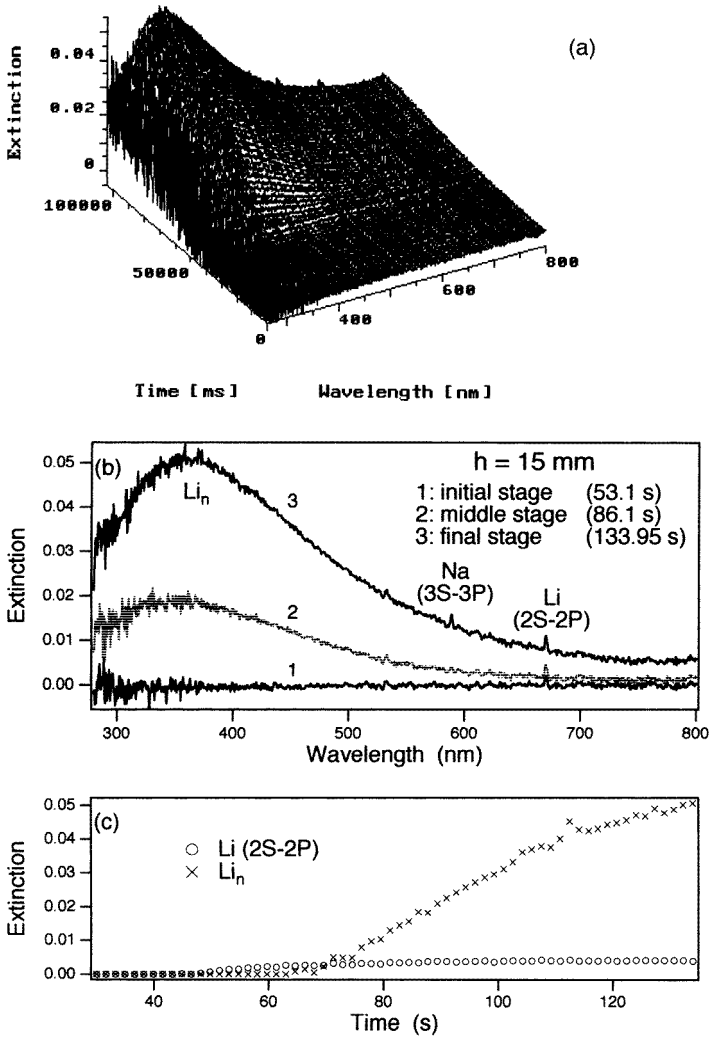

Figure 3. Extinction spectra of the lithium vapour zone at a height of 15 mm from the crucible: (a) time evolution of the extinction spectrum; (b) extinction spectra at the initial, middle and final stages of evaporation; (c) the time dependences of the extinctions due to lithium atoms and clusters.

at each stage were about 604, 694 and 720 K. At the initial stage of the gas evaporation, only a sharp absorption line for Li appears at about 670.7 nm. This wavelength is close to the reported value (White 1934, Phelps 1982) which is due to the 2S–2P electronic transition in atomic lithium. With evaporation in progress, broad absorption bands with fine structures appear at wavelength regions from 600 to 800 nm and from 450 to 550 nm. By referring to a spectroscopic table (Rosen 1970), the former and the latter are assigned to the X–A and X–B electronic–vibrational transitions in the lithium dimer Li_2, respectively. Also, another very broad band is observed at 337 nm. This band is assigned to the collective mode resonance of valence electrons in lithium clusters Li_n ($n > 2$) (Brechignac *et al* 1993). Since the vapour zone at 3 mm was almost transparent as shown in figure 1, it may be

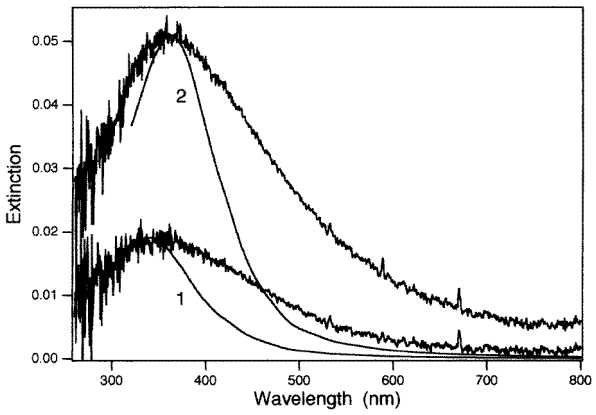

Figure 4. Calculated extinction cross sections of lithium spheres of diameter 31 nm (curve 1) and 51 nm (curve 2), compared with the experimental extinction spectra (curves 2 and 3 of figure 3(b)).

assumed that the lithium clusters in this zone are small clusters. In those spectra, the D line of impurity sodium appears at about 589 nm.

Figure 3(a) shows the time evolution of the extinction spectrum of the blue zone at a height of 15 mm from the crucible edge at 150 Torr. The measurements started 30 s after the beginning of the heating. In figure 3(b), the spectra at initial, middle and final stages are shown. The times indicated are the times elapsed after the beginning of the heating. During the gas evaporation, the temperatures of the measured zone at each stage were about 494, 547 and 566 K. At the initial stage of the gas evaporation, only a sharp atomic absorption line due to the 2S–2P transition appears at about 670.7 nm. With progressive evaporation, broad absorption due to the collective mode resonance of valence electrons in lithium clusters becomes prominent and the resonance wavelength shifts from 335 to 362 nm during evaporation. Unlike the clusters at 3 mm, the clusters at a height of 15 mm may be larger clusters (so-called microcrystals), since we observed considerable smoky light scattering as shown in figure 1. Because, unfortunately, we have no method for determining the sizes of such free microcrystals *in situ*, we estimated the sizes by calculating the extinction cross section of spherical microcrystals, as in previous studies (Mochizuki and Ruppin 1993, 1994). For these calculations we have employed the values of the frequency dependent complex dielectric constant of lithium as measured by Inagaki *et al* (1976). These, however, refer to the bulk, and for small spheres have to be modified so as to account for the free-path effect, which leads to an increase of the imaginary part of the dielectric constant. For this size dependent correction the form suggested by Kreibig (1974) has been used. In the calculations we varied the sphere size, until the peak positions agreed with those of curves 2 and 3 of figure 3(b). Since the number of the microcrystals contributing to the extinction is not known, we have scaled the theoretical curves, so that the heights of the maxima coincide with the experimental ones. The results, shown in figure 4, indicate that the microcrystals had an average size of about 31 nm (curve 1) at the middle stage, and about 51 nm (curve 2) at the final stage. The extinction cross sections are expressed in units of the geometric cross section. The experimental extinction peaks are much broader than calculated ones, because of the size and shape distributions which inevitably exist in the experiment.

In figures 2(c) and 3(c), the time dependences of the extinctions due to atoms, dimers

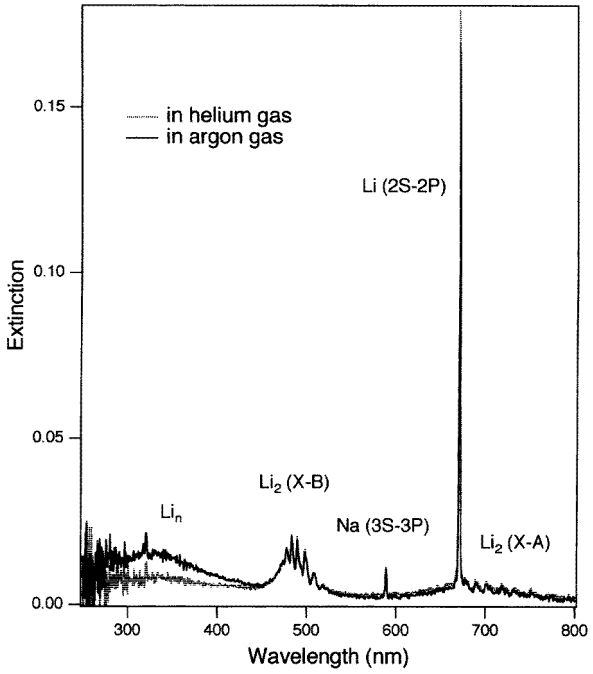

Figure 5. Extinction spectra of the lithium vapour zone at a height of 3 mm produced in the helium and argon gases confined at 150 Torr.

and clusters are plotted for each height. The abscissa corresponds to the times elapsed after starting the heating. These results indicate that lithium atoms evaporate first from the surface of the melt and then coalesce to produce dimers, clusters and microcrystals.

As regards the gas evaporation method, it is frequently stated that a heavier atmospheric gas promotes easier aggregation, since a heavier gas may yield a more efficient confinement of vapour species to the growth region near the vapour source (Granqvist and Buhrman 1976). In order to confirm this optically *in situ*, we carried out comparative experiments at the same evaporation conditions in helium and argon gases which were confined at 150 Torr. The results are shown in figure 5. The extinction spectra were measured at a height of 3 mm. Evidently, an argon gas atmosphere gives more intense extinction due to clusters than a helium one.

From gas evaporation experiments on various kinds of metal, we know that free microcrystals can be produced by evaporation in a moderate pressure gas stream. Figure 6(a) shows the time evolution of extinction due to the collective mode resonance of lithium microcrystals at a height of 5 mm from the crucible edge. The evaporation was carried out in a stream of helium gas with a pressure less than 1 Torr and a flow rate of 5 l min^{-1}. Figure 6(b) and (c) shows the time dependences of the peak energy and the width of the collective mode resonance band. During the measurements, the temperature at a height of 5 mm varied from about 650 K to about 660 K. The decrease of the peak energy and width is due to the size increment of clusters. In the present experiments, the blue shift with increasing size (for very small clusters) due to the electron spillout effect was not observed clearly. Theoretical simulations with the Mie scattering formula were also carried out. The results are shown in figure 7 and indicate that during the times corresponding to those shown in figure 6(b), the average microcrystal radii varied from about 12 nm to about 16 nm.

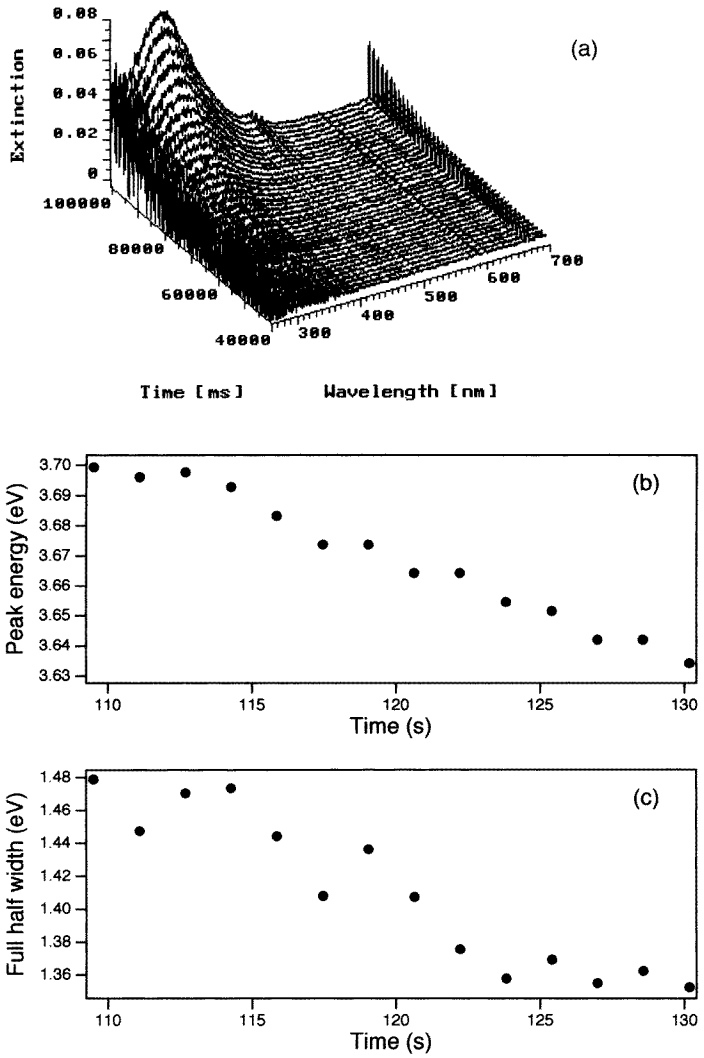

Figure 6. Time evolution of the collective mode resonance band in lithium microcrystals (a) and time dependences of the intensity peak energy (b) and width (c).

3.2. Selective excitation of lithium dimers in vapour

We excited lithium dimers in the dark faint red zone by the 457.9, 476.5, 488.0 and 514.5 nm lines emitted from a CW argon ion laser, and obtained the fluorescence spectra. The results are shown in figure 8.

The emission spectra were obtained at the steady state of gas evaporation. The condition for the gas evaporation was the same as that for the extinction measurements. The broad emission band with sharp fine structures is due to the B–X transitions. A weak emission band due to the A–X transitions is also observed. With decreasing wavelength of the excitation light, the emission band broadens. This may be due to the anharmonicity of the adiabatic potential curves of X and B states.

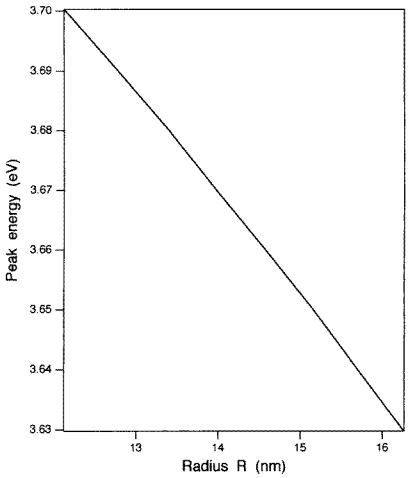

Figure 7. The calculated peak energy of the collective mode of lithium spheres as a function of the radius.

The light-excited dimers may deexcite to emit light, or to dissociate or transfer their excitation energies to nearby atoms, dimers and clusters through collisions. Therefore, under light excitation of dimers, atomic emission lines may be observed simultaneously. Certainly, we can see a sharp atomic line at 670.7 nm. The intensity ratio of atomic emission to dimer emission increases with decreasing wavelength of the excitation light. The ratio is sensitive to the position of measurement and the conditions for gas evaporation. The atomic emission may arise from the appearance of the excited atoms due to predissociation of the excited lithium dimers in the B state $^1\pi_u$ (Mulliken 1932). The predissociation of a dimer in the B state produces both a ground state atom and an excited state atom:

$$\text{Li dimer}(^1\pi_u) \rightarrow \text{Li(2S)} + \text{Li(2P)}. \tag{1}$$

Also, the time evolution of the emission spectrum of the same zone was measured under 457.9 nm excitation. At the initial stage of gas evaporation, the intensity due to atoms prevails against that due to dimers. However, on progression of evaporation, this intensity relation is reversed. Since, at the initial stage of evaporation, the number of atoms is larger than that of dimers, the excitation-energy transfer from light-excited dimers to environmental atoms may be more probable than that to environmental dimers. With further progression of gas evaporation, the concentration of environmental dimers increases and therefore reversal may occur, since the collision cross-section between dimers is larger than that between dimer and atom.

3.3. Selective excitation of lithium clusters in vapour

Valence electrons in clusters oscillate collectively under light illumination and absorb light quanta. The absorption shows a broad intense band. It has been accepted that the broad band width originates from the scattering at the cluster surface, electron–electron scattering and electron–phonon scattering. If such scatterings occur in clusters, we may observe some broadening in the resonance light-scattering spectra. We excited lithium clusters by using the 337 nm nitrogen laser line, which corresponds well to the peak wavelength of the broad collective mode resonance band and observed the light scattering from the clusters. The

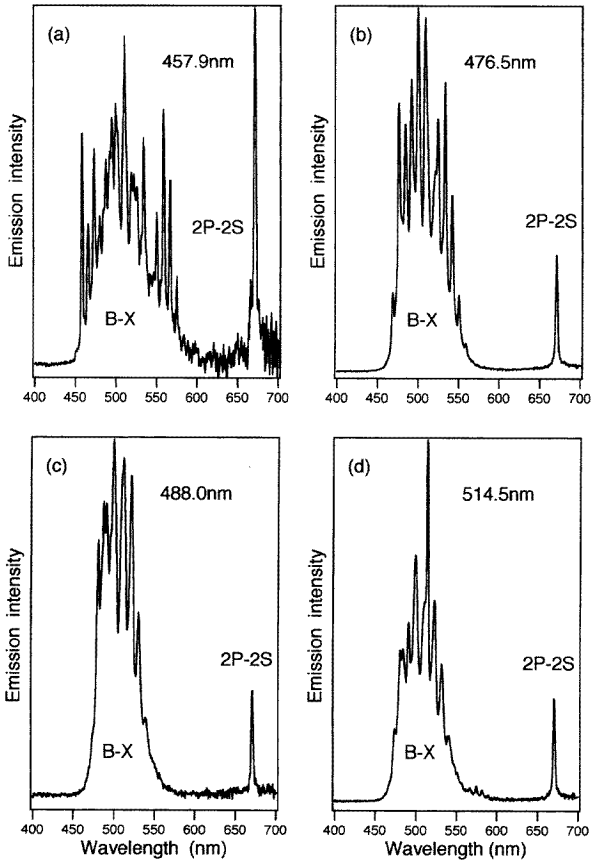

Figure 8. Photoluminescence spectra of lithium dimers for various excitation wavelengths (λ): (a) 457.9 nm; (b) 476.5 nm; (c) 488.0 nm; (d) 514.5 nm.

result is shown in figure 9, together with the excitation laser spectrum. The scattered light was polarized normally to the scattering plane. As shown in this figure, any broadening and any side band could not be observed within the experimental error. From the viewpoint of particle excitation, this may indicate that the large width of the collective mode resonance band of lithium clusters is associated with many transitions of electrons from filled states to many close excited ones between which the electric dipole transitions are forbidden.

3.4. Laser photofragmentation spectroscopy of lithium vapour

We measured the emission spectra of the vertically well separated lithium vapour zones in helium atmosphere confined at 150 Torr at different heights after pulsed-laser-light irradiation. The conditions of the measurements were as follows. The spectra at the heights of 3 and 12 mm are shown in figure 10(a) and (b), respectively. As shown in these figures, we observed sharp lines at about 612 nm and about 673 nm, which are assigned to the 3D–2P and 2P–2S transitions in neutral atoms, respectively. Also, we observed a broad band at about 500 nm which is assigned to the B–X transition in lithium dimer Li_2. With increasing height up to the blue zone, the emission intensities increase. By changing the helium gas to argon, it is found that the emission intensities increase, but the spectral features are

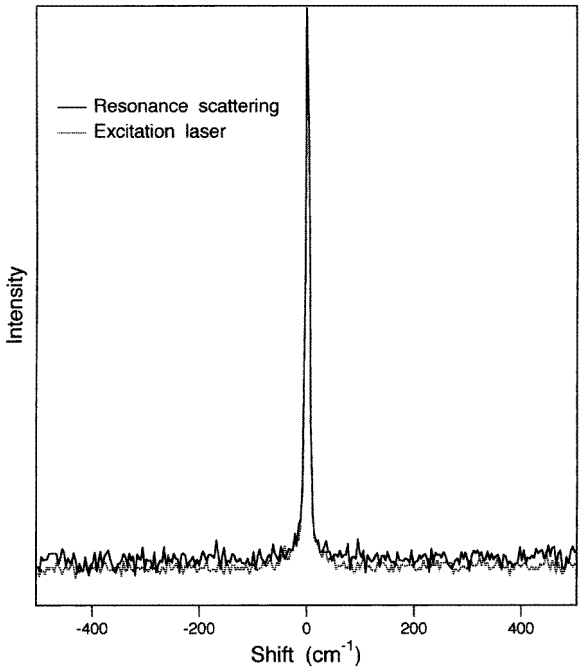

Figure 9. Resonance scattering spectrum of lithium clusters. The excitation laser spectrum is shown by the dotted curve.

scarcely changed. Although the diffuse-band emissions were clearly observed in sodium, potassium and rubidium vapour phases, we have not observed any diffuse-band emission from excimer-like dimers which may originate from lithium trimers ($Li_3 \rightarrow$ excimer-like Li_2+Li). This indicates that the number of lithium trimers is negligibly small in the present vapour zones.

The results obtained are summarized briefly as follows.

(i) In the laser photofragmentation of lithium vapour, emissions from variously excited atoms and lithium dimers are observed.

(ii) The spectral features are independent of the kind of atmosphere, but the emission intensity increases when the helium gas is replaced by argon.

Since we used the 1.06 μm laser line for the excitation, only clusters can be photo-excited electronically through the weak absorption at the long-wavelength tail of the collective mode resonance band. The energy absorbed is then distributed to vibrational modes in the clusters and it concentrates in a special vibrational mode to evaporate atoms and smaller clusters because of the small number of degrees of freedom and small heat capacity. However, since the laser pulse duration is long, the smaller clusters evaporated may be subsequently heated optically by the laser and fragment to produce atoms. At present, it is not clear whether dimers are produced directly through photofragmentation or through aggregation of atoms in the vapour phase. In any case, the result (i) may indicate that, under intense laser-light excitation, clusters in vapour fragment to excited atoms at least. Result (ii) indicates that heavier atmospheric gas effectively confines or deexcites the plume.

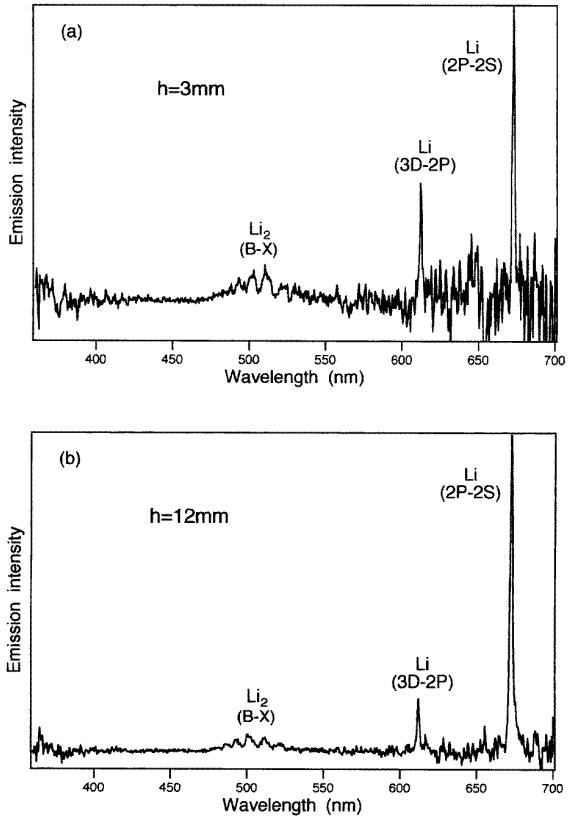

Figure 10. Laser photofragmentation spectra of vapour zones for different heights (h): (a) 3 mm; (b) 12 mm.

3.5. Miscellaneous

3.5.1. The temperature of lithium vapour zones. As described in section 2.1, the temperature corresponding to each spectrum of the vapour zones was measured with a thermocouple. We have previously measured the temperatures of vapour zones for various metals as functions of the height from the crucible and the time elapsed after starting of heating. The results indicated that temperature varied smoothly with increasing time and height. In figures 11(a) and (b), some of the temperatures of lithium vapour zones are shown, so as to correspond to the extinction spectra. V_a is the voltage applied to the crucible heater. The temperatures thus determined may correspond exactly to that of the atmospheric gas. However, it is not clear whether the temperatures are those of vapour species or not, and why the vertically well separated zones are produced without any temperature drop at the zone boundary. In the silver vapour case, we have already explained the formation of the zone structure with a model similar to the liquid drop model for nuclei (Mochizuki and Ruppin 1993), without introducing any temperature drop. However, the ambiguity in true temperatures of vapour species still remains. In spite of temperatures higher than the lithium melting point (452 K), the collective mode resonance was clearly observed. At present, we cannot know whether cluster temperatures are lower than those measured with the thermocouple, or whether the collective mode resonance appears also in the liquid state.

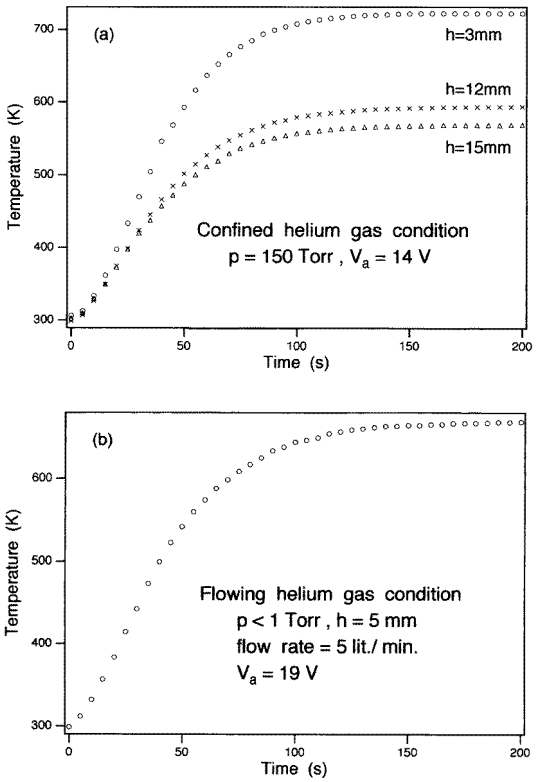

Figure 11. The temperature variation of vapour zones: (a) confined helium gas condition; (b) flowing gas condition.

3.5.2. The electron effective mass of lithium. Lithium metal consists of the atoms having the smallest number of electron which crystalize in a base-centred cubic lattice. The calculation of the electronic structure of solid lithium shows a large energy gap (2.72 eV) at the symmetry point N at which electrons have P-wave character, and the Fermi energy is 3.4 eV (Inoue *et al* 1971, Yamashita 1973). Conduction electrons originate from 2S and 2P states and have a large optical effective mass ($1.28\ m_0 < m^*_{opt} < 1.8\ m_0$) (Inagaki *et al* 1976, Rasigni and Rasigni 1977) and thermal one ($m^*_{th} = 2.3\ m_0$) (Ashcroft and Mermin 1976). However, the optical values spread considerably. It is of interest to deduce the electron effective mass m^* from the highest peak energy 3.7 eV shown in figure 6(b), through the following expression for a spherical microcrystal:

$$\omega_r^2 = 4\pi n e^2/3m^* \tag{2}$$

where ω_r and n are the collective mode resonance frequency and electron density, respectively. The value thus obtained is $1.7\ m_0$, which is close to the value of $1.8\ m_0$ obtained by Rasigni and Rasigni (1977).

References

Ashcroft N W and Mermin N D 1976 *Solid State Commun.* (Philadelphia, PA: Saunders)
Brechignac C, Cahuzac Ph, Leygnier J and Sarfati A 1993 *Phys. Rev. Lett.* **70** 2036
Granqvist C G and Buhrman R A 1976 *J. Appl. Phys.* **47** 2200

Inagaki T, Emerson L C, Arakawa E T and Williams M W 1976 *Phys. Rev.* B **13** 2305
Inoue S T, Asano S and Yamashita J 1971 *J. Phys. Soc. Japan* **30** 1546
Kreibig U 1974 *J. Phys. F: Met. Phys.* **4** 999
Mochizuki S 1993 *Phys. Lett.* **176A** 382
Mochizuki S and Ruppin R 1993 *J. Phys.: Condens. Matter* **5** 135
——1994 *J. Phys.: Condens. Matter* **6** 7303
Mochizuki S and Sasaki M 1995 *Proc. Int. Symp. on the Science and Technology of Atomically Engineered Materials (Richmond, USA, 1995)* ed P Jena, S N Khanna and B K Rao (Singapore: World Scientific) pp 441–6
——1996 *Abstract 51st Ann. Meeting Phys. Soc. Japan* part 2 (Tokyo: Physical Society of Japan)
Mulliken R S 1932 *Rev. Mod. Phys.* **4** 1
Phelps F M III 1982 *M. I. T. Wavelength Tables* (Cambridge, MA: MIT Press)
Rasigni M and Rasigni G 1977 *J. Opt. Soc. Am.* **67** 54
Rosen B 1970 *Spectroscopic Data Relative to Diatomic Molecules* (Oxford: Pergamon)
Ueda R 1974 *J. Cryst. Growth* **24/25** 69
White H E 1934 *Introduction to Atomic Spectra* (New York: McGraw-Hill)
Yamashita J 1973 *Kotai Densiron* (Tokyo: Asakura Syoten) (in Japanese)